Strangeonium Spectroscopy at the J/ψ: A Comparison with Kaon Hadroproduction*

B. N. RATCLIFF

Stanford Linear Accelerator Center
Stanford University, Stanford, California 94309

ABSTRACT

An experimental program to study strangeonium mesons produced in the decays of the J/ψ at a τ-charm factory is compared with experiments on similar final states in kaon hadroproduction. The sample sizes and experimental performance required are discussed. The complementarity of different production modes and the importance of a broad programmatic approach to this physics are stressed.

* Work supported by the Department of Energy under contract No. DE-AC03-76SF00515.

1. INTRODUCTION

The tau-charm factory opens a new window on the high statistics frontier, and will allow the study of extremely large data samples containing light mesons via J/ψ decays. A number of other talks at this workshop have already discussed many specific issues, particularly the search for exotic states, which can be addressed by this large body of data; so rather than adding to this long and impressive list, I will indulge in a few, brief, general remarks about $q\bar{q}$ physics and the experimental environment. I will illustrate these remarks using results from hadronic production with LASS,[1-8] and from J/ψ decays with the MARK III.[9-15]

It must be realized at the outset that any attempt to address the questions of hadron spectroscopy will be a major effort requiring very high quality experiments and extensive analysis of massive data samples. After all, this physics has been studied for well over 20 years in many different production environments and, in many cases, with very large data samples. The candidate theory for strong interactions (QCD) has been under development since the early 1970s, but it is still not possible to calculate the spectrum reliably. Our theoretical understanding of the $q\bar{q}$ hadronic structure remains based largely on "new" versions of old-fashioned constituent quark models,[16] very similar to those which have been in existence for about 25 years. In these circumstances, it seems fair to ask whether the pursuit of this physics justifies the effort.

At the moment, I believe that the answer to this question is a "qualified" yes. One of the clearest predictions of QCD is that exotic hadrons should exist in addition to those predicted by the naive quark constituent quark models. Thus, the presence or absence of these states is a crucial qualitative test of the theory. None of these predicted exotics have been unambiguously identified to date. Since most of these states can hide in amongst the normal $q\bar{q}$ states of the spectrum, it is very important to provide an accurate template of $q\bar{q}$ states to compare against any exotic candidates.

In general, the $q\bar{q}$ spectra are known to agree very well with the simple models

and, in particular, the qualitative features seem clear. More data would clearly help. For example, the orbital excitations are known to lie on linear trajectories; the $L \cdot S$ triplet splittings seem to be small; nonets are approximately magically mixed (except for the ground state); $SU(3)$ predicts the decay rates rather well; etc. However, in many cases (particularly for the $s\bar{s}$ sector), much more data is needed to confirm these features and to provide more direct information to the modelers.

In the future, one hopes that high quality calculations of the QCD spectrum will eventually become available (perhaps from the lattice), so that quantitative comparisons with the experimental spectrum will become a good test of the theory. In this case, we will clearly need very high quality experiments of the kind that can only be provided by a large programmatic approach. Ultimately, progress in this area is likely to depend on a community of theorists and experimentalists interacting over the long term. In particular, a broad spectrum of experimental approaches utilizing different production modes of states with many different decay modes will become very important. In this paper, I discuss how $q\bar{q}$ spectroscopy can be studied in the high statistics limit using examples from LASS, and then compare the production of $s\bar{s}$ mesons seen in J/ψ decays with the $s\bar{s}$ states produced in K^-p interactions; finally, I demonstrate how the approaches complement one another.

2. STRANGE SPECTROSCOPY

Before looking in more detail at the strangeonia, it is useful to set the experimental scale by looking at the strange spectrum produced in K^-p interactions, since this demonstrates the level of data and analysis required to reach a reasonable qualitative understanding of a typical $q\bar{q}$ spectrum. Following are a few examples from the LASS study of the $K^\star$ spectrum. Much of this material was dealt with in more detail at this conference in the presentation by Dunwoodie.[17]

The strange mesons provide an excellent laboratory to study a pure $q\bar{q}$ system since there is no isoscalar-isovector mixing and no confusion with pure glueballs.

In particular, the reactions

$$K^- p \to K^- \pi^+ n \tag{1}$$

and

$$K^- p \to \overline{K}^0 \pi^+ \pi^- n \tag{2}$$

are ideal places to study the orbital excitation ladder, and also provide access to the expected underlying states. Reaction (1) has a particularly simple topology, is restricted to the natural spin-parity series, and has a large cross section which is dominated by π exchange at small values of momentum transfer ($t' \equiv |t - t_{min}|$), whereas reaction (2) can couple to both natural and unnatural spin-parities.

The invariant mass distribution for reaction (1) is shown in Fig. 1 for the 730,000 events with $t' \leq 1.0$ GeV/c^2. The spin-parity $J^P = 1^- K^\star(892)$ and $2^+ K_2^\star(1430)$ mesons can be clearly seen, as can a higher mass structure in the $3^- K_3^\star(1780)$ region. Similarly, the invariant mass for the 90,000 events of reaction (2) shown in Fig. 2 has structure in the $K_2^\star(1430)$ and $K_3^\star(1780)$ regions. However, in neither case is there any direct evidence in the mass plots for the higher mass leading resonances nor for the expected underlying states, and at first sight the cross sections appear to be largely background on which the low mass leading resonances are superimposed. Partial wave analyses (PWA) of these data show, however, that the cross sections are composed of many resonances; indeed, even the "obvious" leading structures contain significant contributions from underlying resonances in the same mass regions.

The PWA amplitudes for reaction (1) demonstrate clear Breit–Wigner structures for the leading orbitally excited natural spin-parity states with J^P from 2^+ up to 5^-, as shown in Fig. 3. The $K_2^\star(1430)$, the $K_3^\star(1780)$, the $K_4^\star(2060)$, and the $K_5^\star(2380)$ are clearly seen. Similarly, the same leading natural spin-parity resonances with J^P up to 4^+ can be seen in the natural spin-parity waves of reaction (2), as shown in Fig. 4. There is also substantial structure in the underlying waves as can be seen in the amplitude plots for reaction (1), which are shown in

Fig. 5. There are underlying states in the 0^+ wave around 1.4 and 1.95 GeV/c^2; in the 1^- wave around 1.4 and 1.8 GeV/c^2; and perhaps in the 2^+ wave around 1.9 GeV/c^2. Reaction (2) has similar structures in the 1^- wave around 1.4 and 1.8 GeV/c^2, and in the 2^+ wave around 2.0 GeV/c^2, as seen in Fig. 4.

Detailed analyses of strange mesons in these and other channels from LASS have produced many more results, as discussed elsewhere.[1,2] Figure 6 summarizes the $K^\star$ spectrum observed to date. The observed leading states lie on an essentially linear orbital ladder that extends up through the $5^- K^\star$. Several of the expected triplet multiplets have been seen and there are good candidates for radial states. LASS has measured π transitions from most of these states as well as transitions to vector, and in some cases, tensor and η mesons; in general, the decay rates are consistent with those predicted by SU(3), and the parameters of these states agree well with the predictions of the quark model.[16] The major exception is with the 1^- excited spectrum where the apparent radial state lies below the model predictions in mass. Since this state also has unusual decay rates, in particular, having an elastic rate of only 7%, it points to inadequacies in the models which may result from incomplete treatment of the wavefunction dynamics.[18] However, of most relevence to this talk, we see that a detailed program of analyses in several different final states with very large statistics (ranging up to almost 1 million events), is just barely able to pin down most of the details on the spectrum, including the underlying states. Reaching a similar level of understanding of the $s\bar{s}$ spectrum is likely to require a commensurate effort.

3. STRANGEONIA

The strangeonium mesons are of particular interest since several candidates for exotic mesons, as discussed at this workshop, couple strongly to the same final states. The reactions

$$K^- p \to K^- K^+ \Lambda \tag{3}$$

$$K^- p \to K^0_S K^0_S \Lambda \tag{4}$$

$$K^- p \to K^0_S K^\pm \pi^\mp \Lambda \tag{5}$$

are dominated by peripheral hypercharge exchange which strongly favors the production of $s\bar{s}$ mesons over glueballs. Thus, these channels provide a clear look at the strangeonia, which can provide revealing comparisons with the same final states produced in other channels that might be glue-enriched. Only a very short review of material of direct relevance to $s\bar{s}$ spectroscopy is given here. In the following section, I will compare a few results with production of similar final states from the MARK III. More details of these results are available in published papers.[4-7]

The mass spectrum of Fig. 7(a) for reaction (3) shows bumps corresponding to the known $\phi(1020)$ and $f_2'(1525)$ leading orbital states, as well as a smaller bump in the $\phi_J(1850)$ region. Only the $f_2'(1525)$ is observed in Fig. 7(b) for reaction (4) since it is restricted to even spin states. In neither case is there any evidence for the $\theta(1720)$.

Amplitude analyses of these data (Fig. 8) display the expected P-wave structure for the $\phi(1020)$ and D-wave for the $f_2'(1525)$. In addition, the S-wave intensity [Fig. 8(d)] from reaction (4) appears to peak around the $f_2'(1525)$ mass. Although the errors on the individual points are large (and nonlinear), the data require the existence of an S-wave in this region at about the 5σ level. This suggests the existence of a 0^+ resonance which is most naturally interpreted as the triplet partner of the $f_2'(1525)$,[4] and leads us to suggest that the $f_0(975)$, which is usually assigned to this multiplet, may not be a $q\bar{q}$ state.

The F-wave intensity distribution of Fig. 9(a) shows a structure in the 1850 MeV/c^2 region which can be simply associated with the $\phi_J(1850)$ bump in the mass distribution [Fig. 9(b)]. A Breit–Wigner fit to the F-wave amplitude of Fig. 9(a) gives parameters M=1855 $\pm$ 22, Γ = 74 $\pm$ 67 MeV/c^2, while a fit to the cross section gives M=1851 $\pm$ 7, Γ = 66 $\pm$ 29 MeV/c^2. We have also shown that the interference between $s\bar{s}$ resonance production and diffractive N^* production can be utilized to analyze the leading the $s\bar{s}$ amplitude, and this method gives results consistent with the above for the F-wave.[6] An extension of this method has been utilized to analyze the G-wave amplitude in the 2.2 GeV/c^2 mass region. Figure 10 shows evidence for a 4^+ state [the $f_4'(2210)$] which is a good candidate to be the mainly $s\bar{s}$ member of the 4^{++} nonet predicted by the quark model.

The most prominent features of the $K\overline{K}\pi$ mass distribution [Fig. 11(a)] from reaction (5) are a sharp rise at $K^*\overline{K}$ threshold followed by a peak around 1.5 GeV/c^2, and a second peak around 1.85 GeV/c^2. The PWA shows that the low mass region is dominated by 1^+ K^* waves, while the higher mass structure contains evidence for peaks in the 2^- and 3^- waves. The 1^+ waves can be combined to form eigenstates of G-parity as shown in Fig. 11(b) and 11(c). These distributions are well described by Breit–Wigner curves as shown, and, assuming $I = 0$, provide good evidence for two $s\bar{s}$ axial-vector meson states: one with quantum numbers $J^{PC} = 1^{++}$, M$\sim$ 1530 MeV/c^2, and $\Gamma \sim$ 100 MeV/c^2, and the other with $J^{PC} = 1^{+-}$, M$\sim$ 1380 MeV/c^2, and $\Gamma \sim$ 80 MeV/c^2. These states are good candidates to be the mostly strangeonium members of the ground state 1^{++} and 1^{+-} nonets predicted by the quark model.

Figure 12 summarizes the strangeonia observed from LASS in the channels just discussed. The general features of the spectrum are reminiscent of the K^* spectrum discussed above. The observed leading states lie on an essentially linear orbital ladder that extends up through the $4^+ f_4'$, and there are good candidates for the triplet partners of the $f_2'(1525)$. Except for the ground state pseudoscalar, the states appear to fit into SU(3) multiplets which are consistent with magic mixing, and the parameters and decay transitions of these states agree well with

the predictions of the quark model.[16,20] However, it must be recognized that this interpretation is an "optimist's" view. The only really well-measured states are the $J^P = 1^-, 2^+, 3^-$ leading orbital excitations. The next leading state is about a 4σ effect, and we are just beginning to understand underlying states and the triplet splittings.

4. COMPARISON OF DIFFERENT PRODUCTION MODES

As discussed earlier, we expect that in understanding the $s\bar{s}$ sector and the nature of the exotics, it will be important to study several different production modes. To be explicit, it is useful to compare some known features of production via J/ψ decays vs. the same states produced in K^-p interactions. We expect, for example, that (1) radiative J/ψ decays should be glue enriched with respect to objects produced by K^-p recoiling against a Λ, which should be strangeonium enriched; (2) high-spin leading orbital states should be suppressed in J/ψ decays but should be the clearest high mass states seen in K^-p production. Thus, we expect to see many similarities in the physics, but also many differences coming both from the production properties and from quantum number restrictions at production.

To demonstrate these features, it is useful to compare a few results from LASS and the MARK III. For example, if we compare the mass distribution for the reaction

$$K^-p \to K^0_S\, K^0_S\, \Lambda$$

seen in LASS with that from the reaction

$$e^+e^- \to J/\psi \to \gamma\, K^0_S\, K^0_S$$

from the MARK III, as shown in Fig. 13, we see an $f_2'(1525)$ in both modes. However, there is a large $\theta/f_2(1720)$ bump from the MARK III data which does

not exist at all in the LASS data. This leads to the conclusion that the θ is unlikely to be a 2^{++} $s\bar{s}$ meson and is a good candidate to be an exotic. On the other hand, if one compares the mass distributions in the region around 2.2 GeV/c^2, as shown in Fig. 14, the two experiments are consistent in mass shape. Since LASS has been able to show that there is good evidence for a 4^{++} strangeonium object in this mass region as described above, it is at least plausible that the object seen in the MARK III is either the same object or its triplet 2^{++} partner, and an exotic explanation is not required.

In a similar way, we can compare the mass distribution observed in LASS for reaction (3), as shown in Fig. 7(a), with those from the reactions

$$e^+e^- \rightarrow J/\psi \rightarrow \gamma\ K^+\ K^-$$
$$e^+e^- \rightarrow J/\psi \rightarrow \omega\ K^+\ K^-$$
$$e^+e^- \rightarrow J/\psi \rightarrow \phi\ K^+K^- \quad ,$$

as seen by MARK III in Fig. 15. The three leading orbital excitations are clearly seen as bumps in the LASS distributions and there is no clear evidence of $f_2(1720)$. In contrast, there are provacative differences between the different tagged samples from the MARK III, and, in particular, there is some evidence for $f_2(1720)$ in all three distributions. Other examples of comparisons between data from these experiments have been made at this workshop by several speakers. In the interest of brevity, I refer the interested reader there.[17,19]

For the future, it is of particular interest to compare experiments that might be performed at a tau-charm factory with those that might be performed at a kaon factory. A recent study of feasible experiments at KAON[21] concluded that it would be possible to perform a "LASS-style" experiment to study $s\bar{s}$ physics with approximately 100 times LASS statistics, while an experiment with 1000 times the present MARK III data set should be feasible at the tau-charm factory. As can be seen from Table I, at present, in a given channel LASS typically has an advantage in statistics of ~ 3, although this is quite channel dependent.

Table I

Comparison of observed event rates in e^+e^- and K^-p production for several different hadronic final states. The recoil particle is indicated in parentheses. The observed events are those seen in e^+e^- by the Mark III and in K^-p interactions with LASS. The projected events are as might be expected from large scale experiments at a tau-charm factory and at a kaon factory (see text).

	OBSERVED EVENTS		PROJECTED EVENTS	
FINAL STATE	MARK III	LASS	TAU-CHARM 1000× Mark III	KAON 100× LASS
K_sK_s	(γ) 590	(Λ) 411	$(\gamma)\ 6\times10^5$	$(\Lambda)\ 4\times10^4$
K^-K^+	(γ) 4400 (ϕ) 320	(Λ) 12294	$(\gamma)\ 4\times10^6$ $(\phi)\ 3\times10^5$	$(\Lambda)\ 1.2\times10^6$
$K^{*0}\ \overline{K}^{*0}$	(γ) 811	(Λ) 1650	$(\gamma)\ 8\times10^5$	$(\Lambda)\ 2\times10^5$
$K\overline{K}\pi$	(ϕ) 670	(Λ) 3900	$(\phi)\ 7\times10^5$	$(\Lambda)\ 4\times10^5$

Moreover, LASS has a flatter acceptance than the MARK III and so is superior for performing detailed PWA of the data. However, a new detector for the tau-charm factory should eliminate this advantage for the fixed target work, so that by the next generation, e^+e^- should be comparable to or superior in both statistics and acceptance to the fixed target experiments. One final comment: even though the projected numbers of events in the final states shown are very large, experience, as described above for the strange channels, has shown that it is essential to have of order $10^5 - 10^6$ events per channel in a high acceptance device in order to be able to perform a full PWA and understand the nature of the underlying states.

5. CONCLUSION

The experimental study of strangeonia produced in J/ψ decays will be an important area for a tau-charm factory. It is essential in the search for exotics, and will also be important in elucidating the properties of the underlying pure $s\bar{s}$ states which have yet to be clearly understood. Experimentally, the production of strangeonia in e^+e^- machines is complementary to production with hadronic beams, and both kinds of experiments, along with more theoretical work, are required in order to finally make definitive tests of QCD calculations of the spectrum. However, such experiments are a substantial effort. They require (1) a very high quality spectrometer with 4π acceptance, full vertex reconstruction, particle identification, γ detection and a high (1 KHz) data-taking rate; (2) very large data samples ($\approx 10^{10}$ events); (3) lots of data storage and CPU horsepower; (4) sophisticated analysis programs; and (5) a committed group of individuals to carry out a long-term program of analysis.

I would like to thank the members of the LASS and MARK III groups, whose work has provided the material for this talk.

REFERENCES

1. D. Aston et al., Nucl. Phys. **B292** (1987) 693.
2. D. Aston et al., Phys. Lett. **180B** (1986) 308; Nucl. Phys. **B296** (1988) 493.
3. D. Aston et al., Phys. Lett. **201B** (1988) 169.
4. D. Aston et al., Nucl. Phys. **B301** (1989) 525.
5. D. Aston et al., Phys. Lett. **201B** (1988) 573.
6. D. Aston et al., Phys. Lett. **208B** (1988) 324.
7. D. Aston et al., Phys. Lett. **215B** (1988) 199.
8. D. Aston et al., "The LASS Spectrometer," SLAC–REP–298 (1986).
9. D. Coffman et al., Phys. Rev. **D38** (1988) 2695.
10. J. Becker et al., SLAC–PUB–4243 (1987).
11. J. Becker et al., Phys. Rev. Lett. **59** (1987) 186.
12. R. Baltrusaitis et al., Phys. Rev. **D35** (1987) 2077.
13. W. Lockman et al., SCIPP 86/87 (1986).
14. U. Mallik et al., SLAC–PUB–3946 (1986).
15. R. Baltrusaitis et al., Phys. Rev. Lett. **56** (1986) 107.
16. See, for example, S. Godfrey and N. Isgur, Phys. Rev. **D32** (1985) 189.
17. W. Dunwoodie, presentation at this workshop.
18. See for example, A. Bradley, J. Phys., **G4** (1978) 1517.
19. G. Eigen, presentation at this workshop.
20. S. Godfrey and N. Isgur, Phys. Lett. **141B** (1984) 439.
21. Proceedings of the Workshop on Hadron Spectroscopy at the KAON Factory, Vancouver, Canada, Feb. 19–21, 1989.

FIGURE CAPTIONS

1) The $K^-\pi^+$ mass distribution from reaction (1); the cross-hatched plot contains events with N^*'s removed ($M(n\pi^+) \geq 1.7$ GeV/c^2).

2) The $\overline{K^0_s}\pi^+\pi^-$ mass distribution from reaction (2) for all events (top plot) and for events with $t' \leq 0.3$ GeV/c^2 (bottom plot); the dashed line gives the final acceptance after all cuts.

3) The leading natural spin-parity resonant amplitudes from reaction (1).

4) The natural spin-parity wave sums from reaction (2).

5) The magnitudes and phases of the amplitudes for solution A for reaction (1); there are two different solutions which are identical below the mass indicated by the broken line.

6) Level diagram summarizing the strange meson states and transitions seen in this experiment.

7) The $K\overline{K}$ mass spectra from: (a) reaction (3); and (b) reaction (4).

8) The low mass $K\overline{K}$ amplitudes from: (a-b) reaction (4); (c-d) reaction (3).

9) The mass region around 1850 MeV/c^2 from reaction (3): (a) the F-wave intensity; (b) the mass dependent total cross section.

10) The mass dependence of the interference between the G_0 and diffractive background amplitudes from reaction (3).

11) The $K\overline{K}\pi$ mass distribution (a) from reaction (5); (b-c) the 1^+ G-parity eigenstate amplitudes.

12) Level diagram summarizing the strangeonium meson states and transitions seen in LASS.

13) A comparison of the K_sK_s mass distributions from LASS and radiative J/ψ decay from the MARK III[15] in the region below 1.9 GeV/c^2; the LASS data have been scaled to match the MARK III data at the $f_2'(1525)$; the large MARK III signal for the $f_2(1720)$ is not present in the LASS data.

14) The acceptance corrected K_sK_s invariant mass distribution in the mass region between 1.8 and 2.7 GeV/c^2 from LASS compared with the same final state as seen by the MARK III.[15]

15) The K^+K^- invariant mass distribution observed by the MARK III in J/ψ decays, tagged by recoil particle; (a) γ; (b) ω; (c) ϕ.

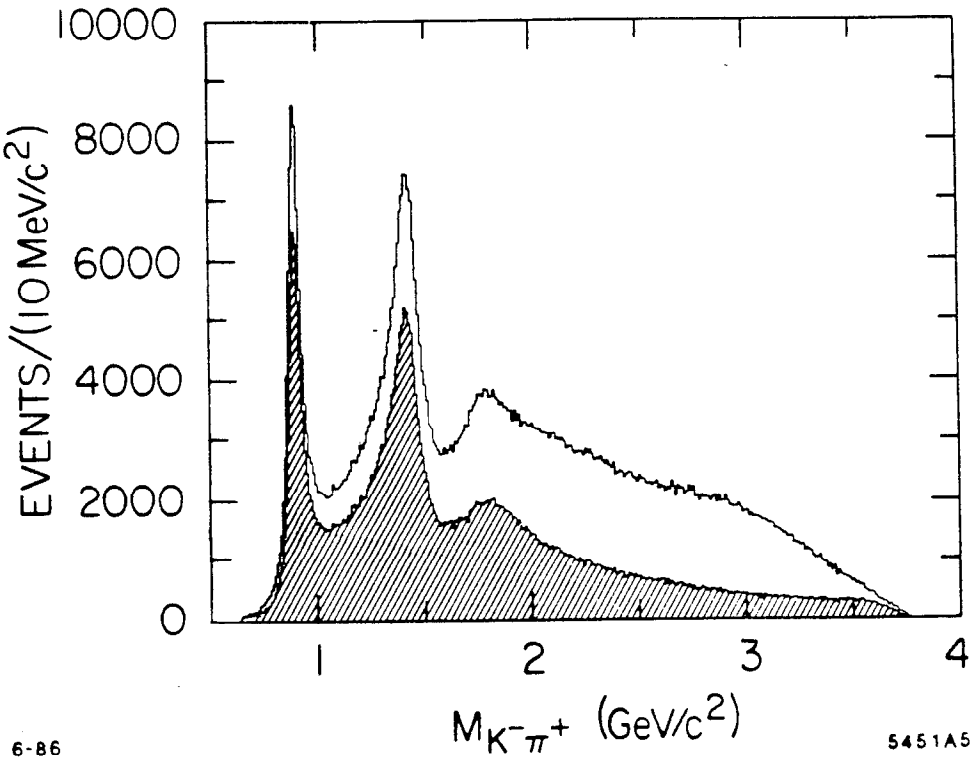
10000
8000
6000
4000
2000
0
EVENTS/(10 MeV/c²)
1
2
3
4
M K⁻π⁺ (GeV/c²)
6-86
5451A5

Fig. 1

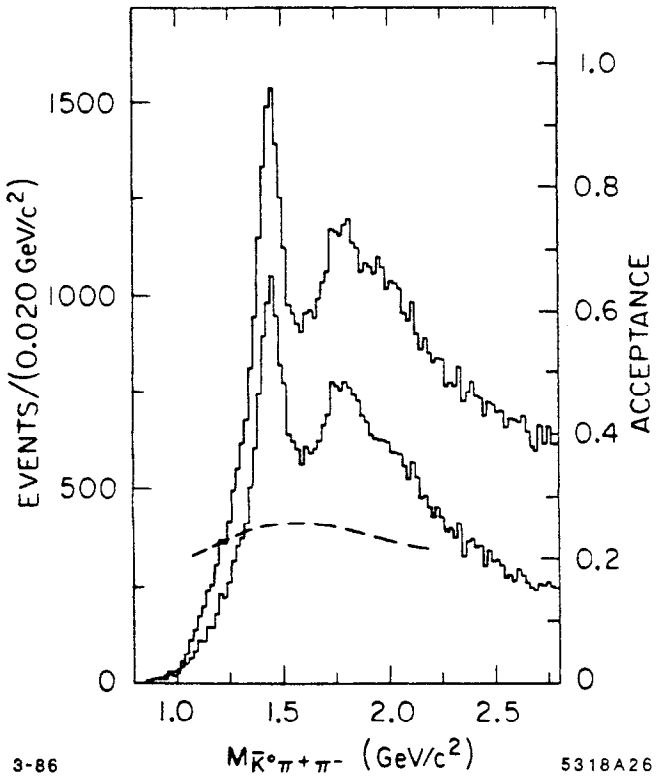
1500
1000
500
0
EVENTS/(0.020 GeV/c²)
1.0
0.8
0.6
0.4
0.2
0
ACCEPTANCE
1.0
1.5
2.0
2.5
M K̄⁰π⁺π⁻ (GeV/c²)
3-86
5318A26

Fig. 2

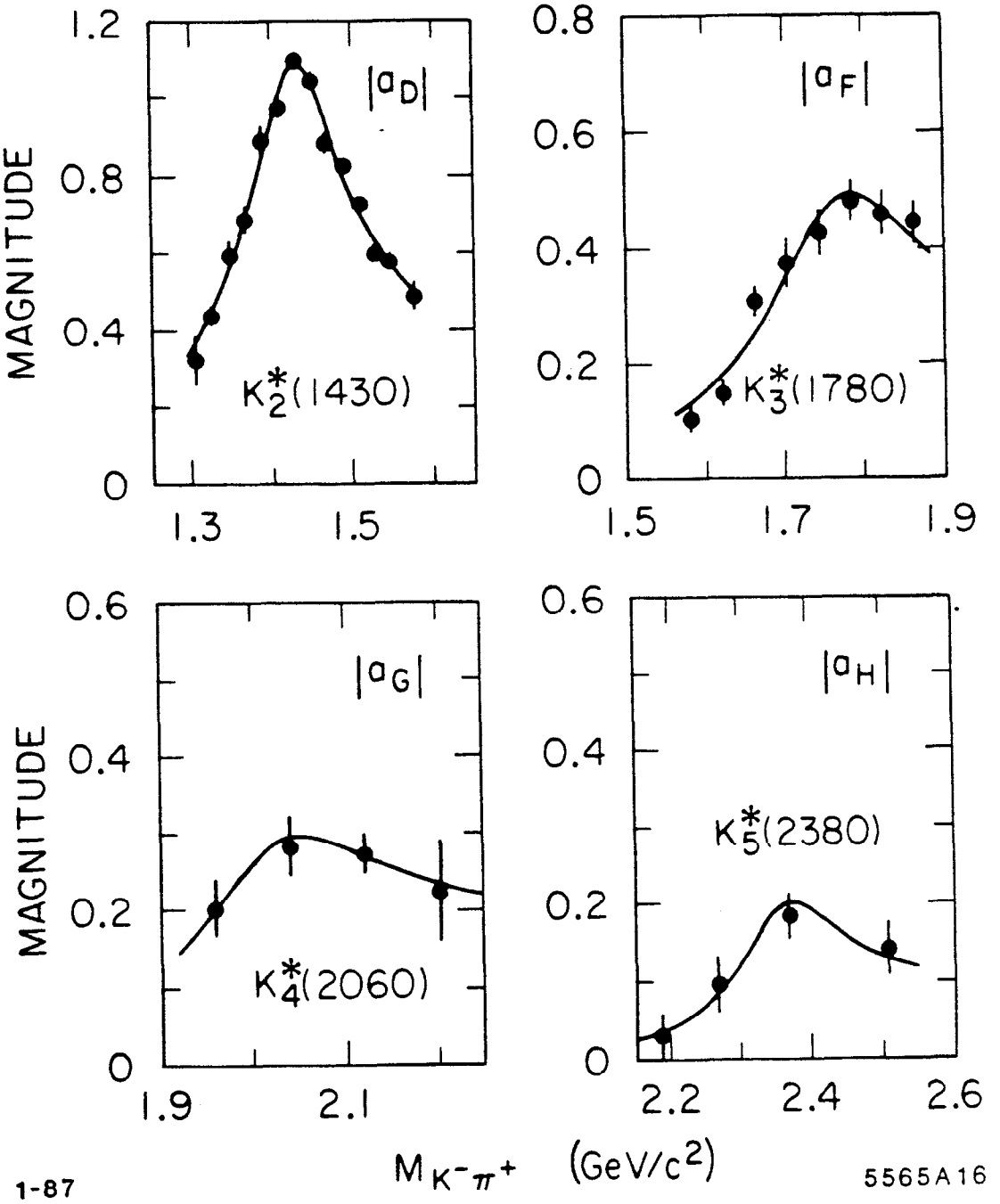
MAGNITUDE
1.2
0.8
0.4
0
$|a_D|$
$K_2^*(1430)$
1.3
1.5
0.8
0.6
0.4
0.2
0
$|a_F|$
$K_3^*(1780)$
1.5
1.7
1.9
MAGNITUDE
0.6
0.4
0.2
0
$|a_G|$
$K_4^*(2060)$
1.9
2.1
0.6
0.4
0.2
0
$|a_H|$
$K_5^*(2380)$
2.2
2.4
2.6
$M_{K^-\pi^+}$ (GeV/c^2)
1-87
5565A16

Fig. 3

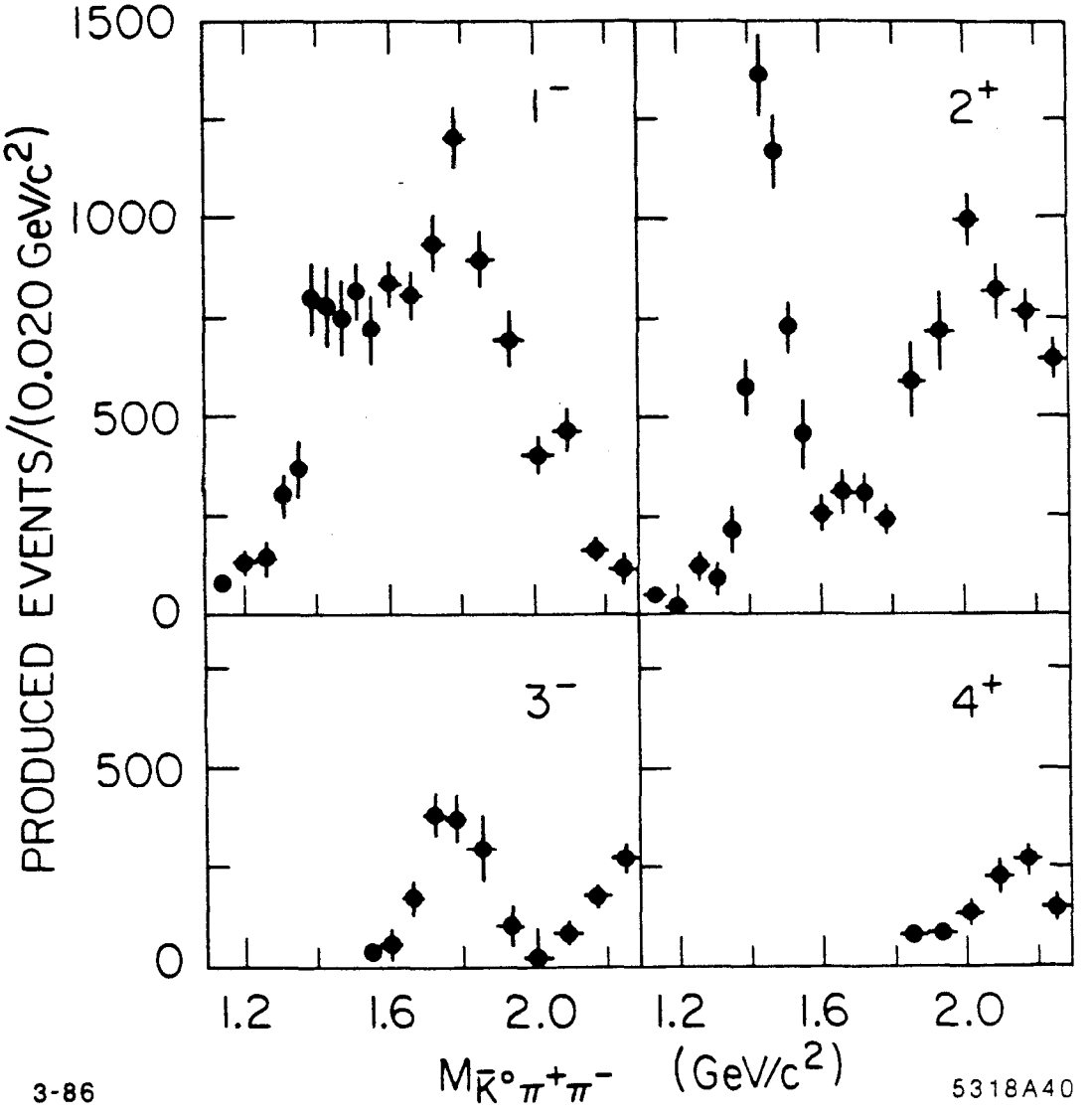
1500
1000
500
0
500
0
PRODUCED EVENTS/(0.020 GeV/c²)
1⁻
2⁺
3⁻
4⁺
1.2
1.6
2.0
1.2
1.6
2.0
M K̄°π⁺π⁻ (GeV/c²)
3-86
5318A40

Fig. 4

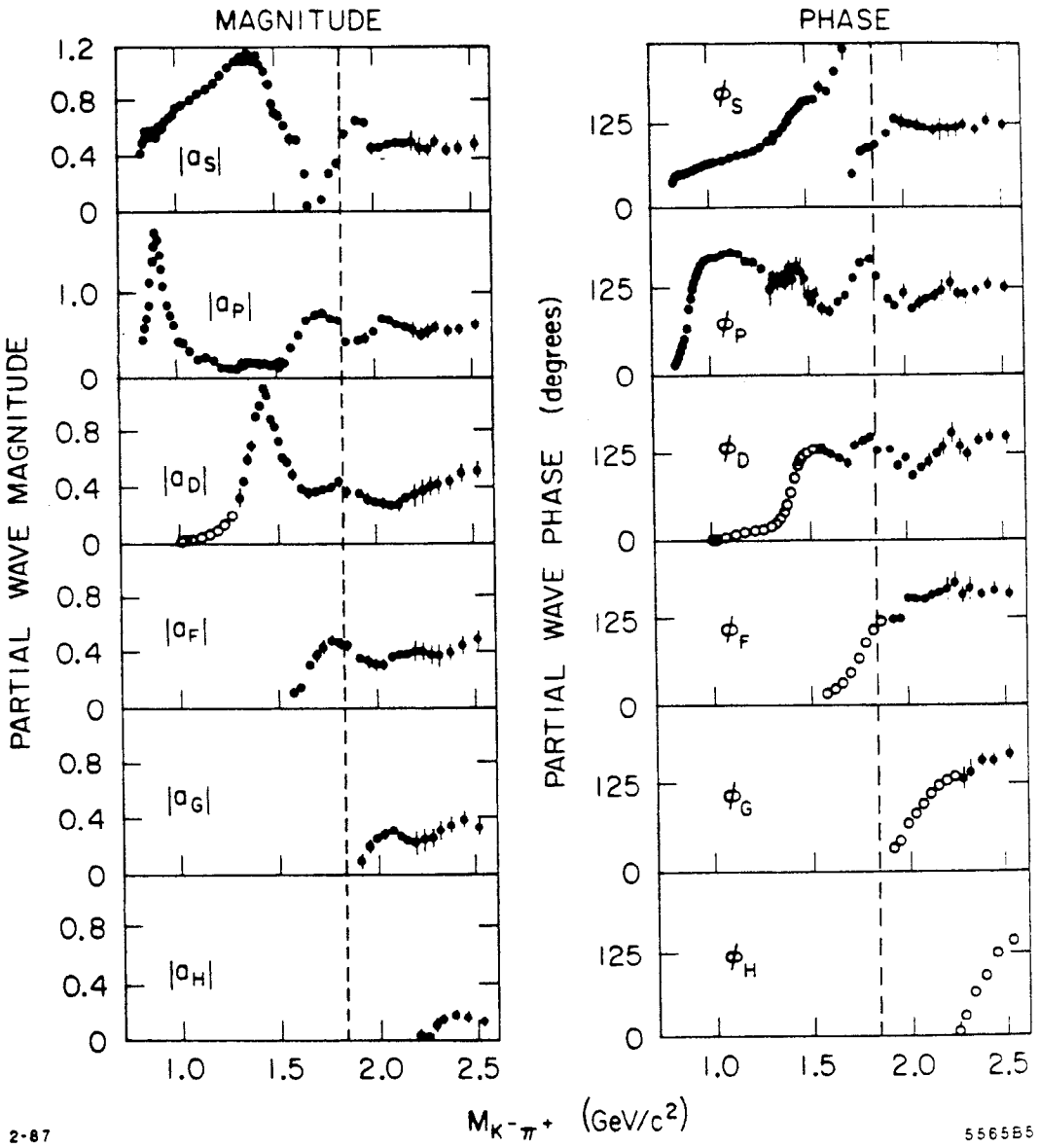
MAGNITUDE
PHASE
PARTIAL WAVE MAGNITUDE
PARTIAL WAVE PHASE (degrees)
$|a_S|$
$|a_P|$
$|a_D|$
$|a_F|$
$|a_G|$
$|a_H|$
ϕ_S
ϕ_P
ϕ_D
ϕ_F
ϕ_G
ϕ_H
$M_{K^-\pi^+}$ (GeV/c^2)
2-87
5565B5

Fig. 5

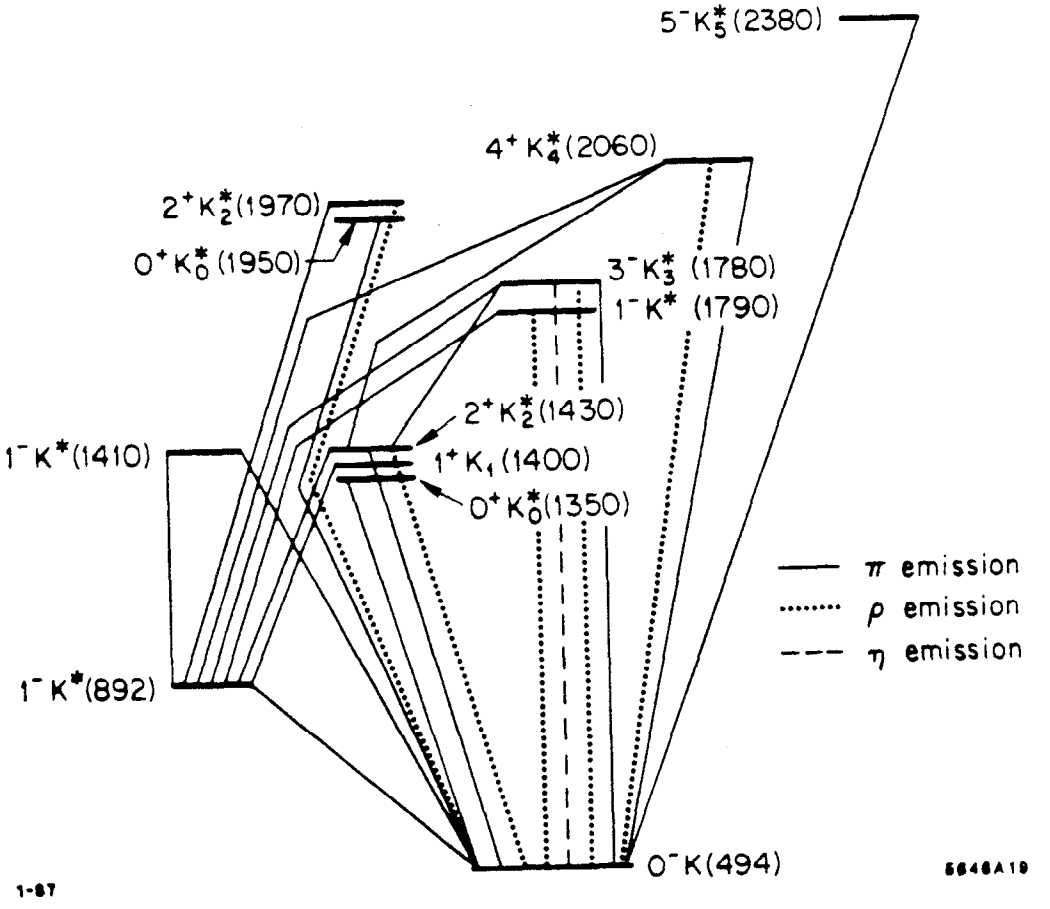
5⁻K*5(2380)
4⁺K*4(2060)
2⁺K*2(1970)
0⁺K*0(1950)
3⁻K*3(1780)
1⁻K*(1790)
2⁺K*2(1430)
1⁻K*(1410)
1⁺K1(1400)
0⁺K*0(1350)
1⁻K*(892)
0⁻K(494)
π emission
ρ emission
η emission
1-87
5646A19

Fig. 6

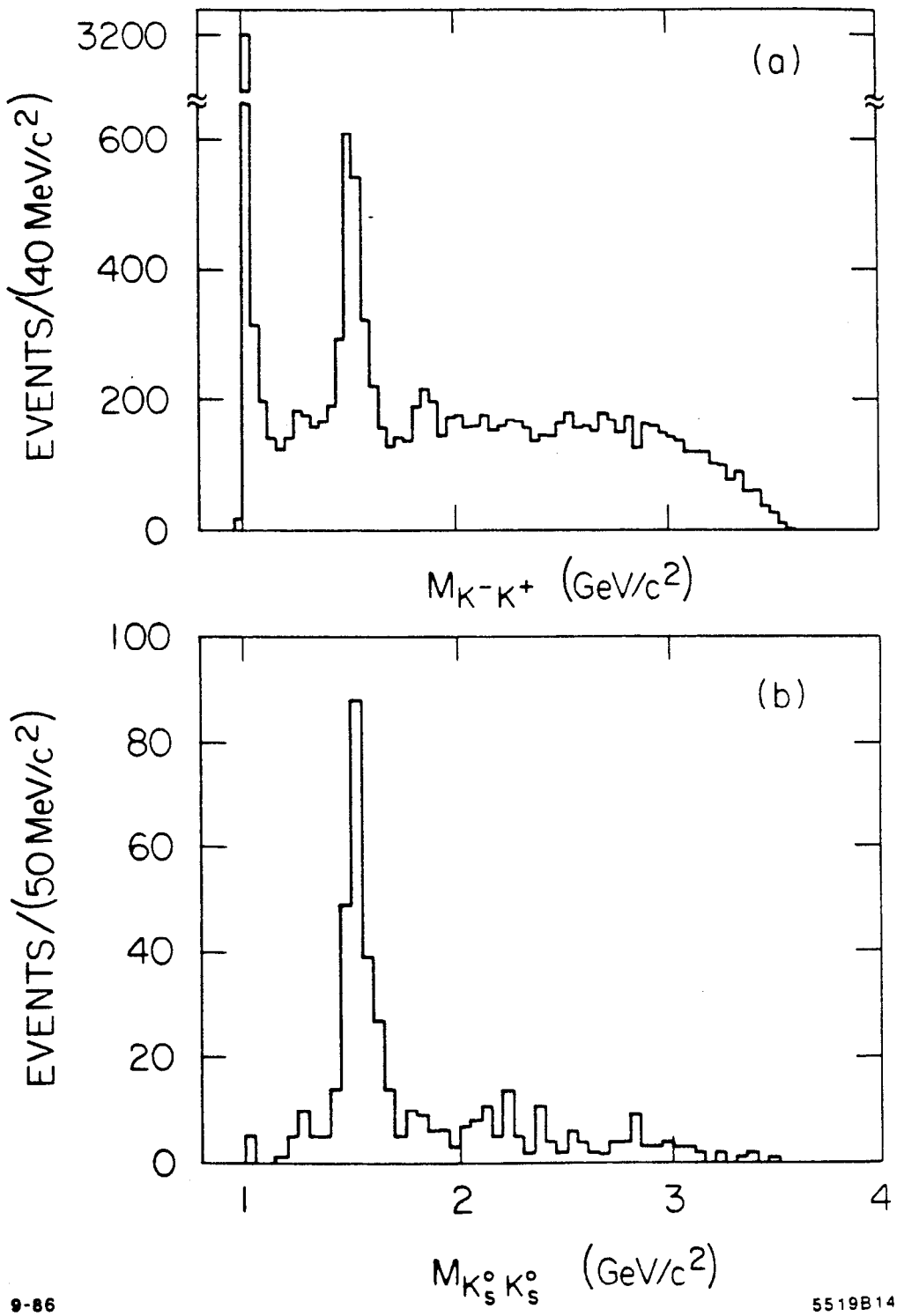
3200
600
400
200
0
(a)
EVENTS/(40 MeV/c²)
M K⁻K⁺ (GeV/c²)
100
80
60
40
20
0
1
2
3
4
(b)
EVENTS/(50 MeV/c²)
M K°s K°s (GeV/c²)
9-86
5519B14

Fig. 7

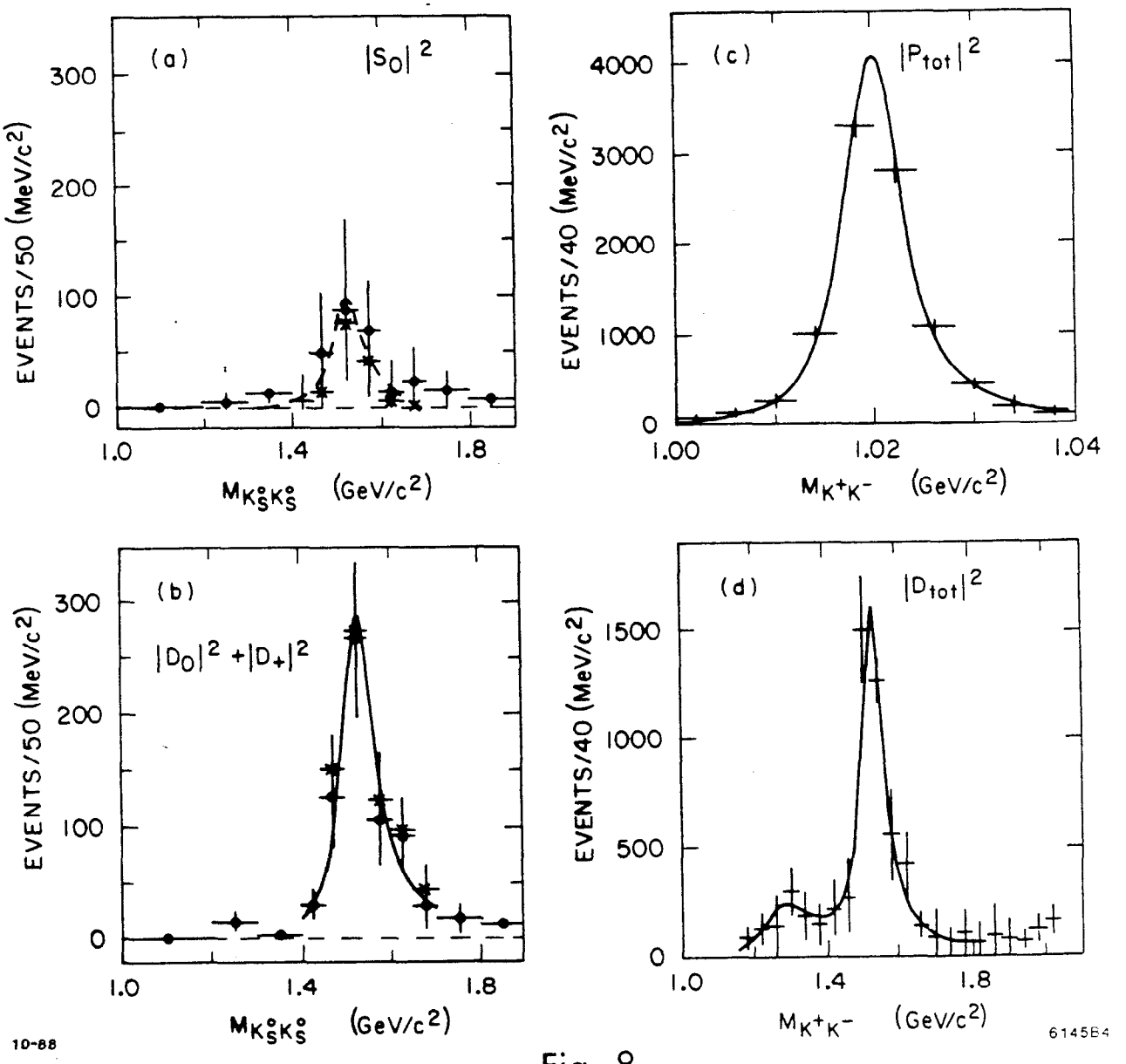
(a)
$|S_0|^2$
EVENTS/50 (MeV/c²)
$M_{K_S^0K_S^0}$ (GeV/c²)
(b)
$|D_0|^2 + |D_+|^2$
EVENTS/50 (MeV/c²)
$M_{K_S^0K_S^0}$ (GeV/c²)
(c)
$|P_{tot}|^2$
EVENTS/40 (MeV/c²)
$M_{K^+K^-}$ (GeV/c²)
(d)
$|D_{tot}|^2$
EVENTS/40 (MeV/c²)
$M_{K^+K^-}$ (GeV/c²)
10-88
6145B4

Fig. 8

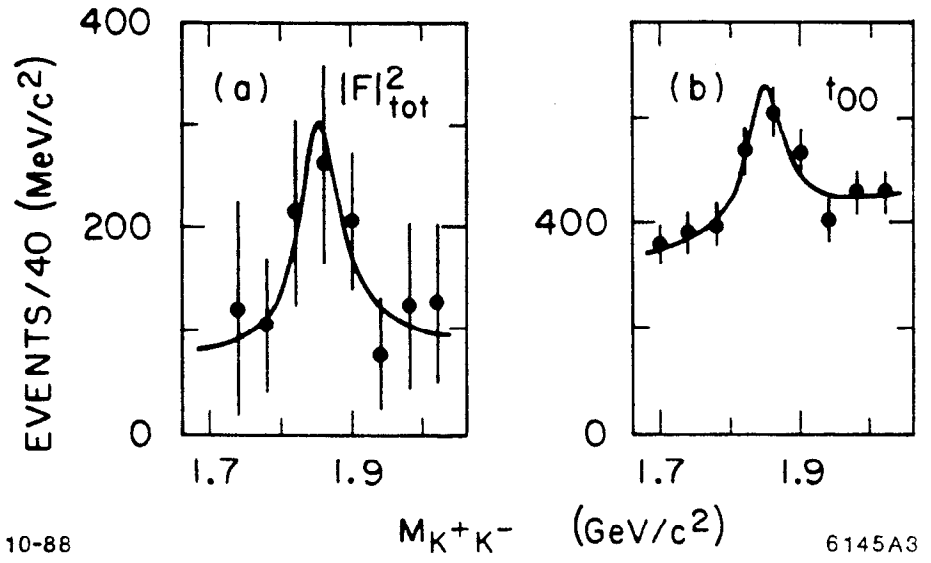
400
200
0
EVENTS/40 (MeV/c²)
(a)
$|F|^2_{tot}$
1.7
1.9
400
0
(b)
t_{00}
1.7
1.9
$M_{K^+K^-}$ (GeV/c²)
10-88
6145A3

Fig. 9

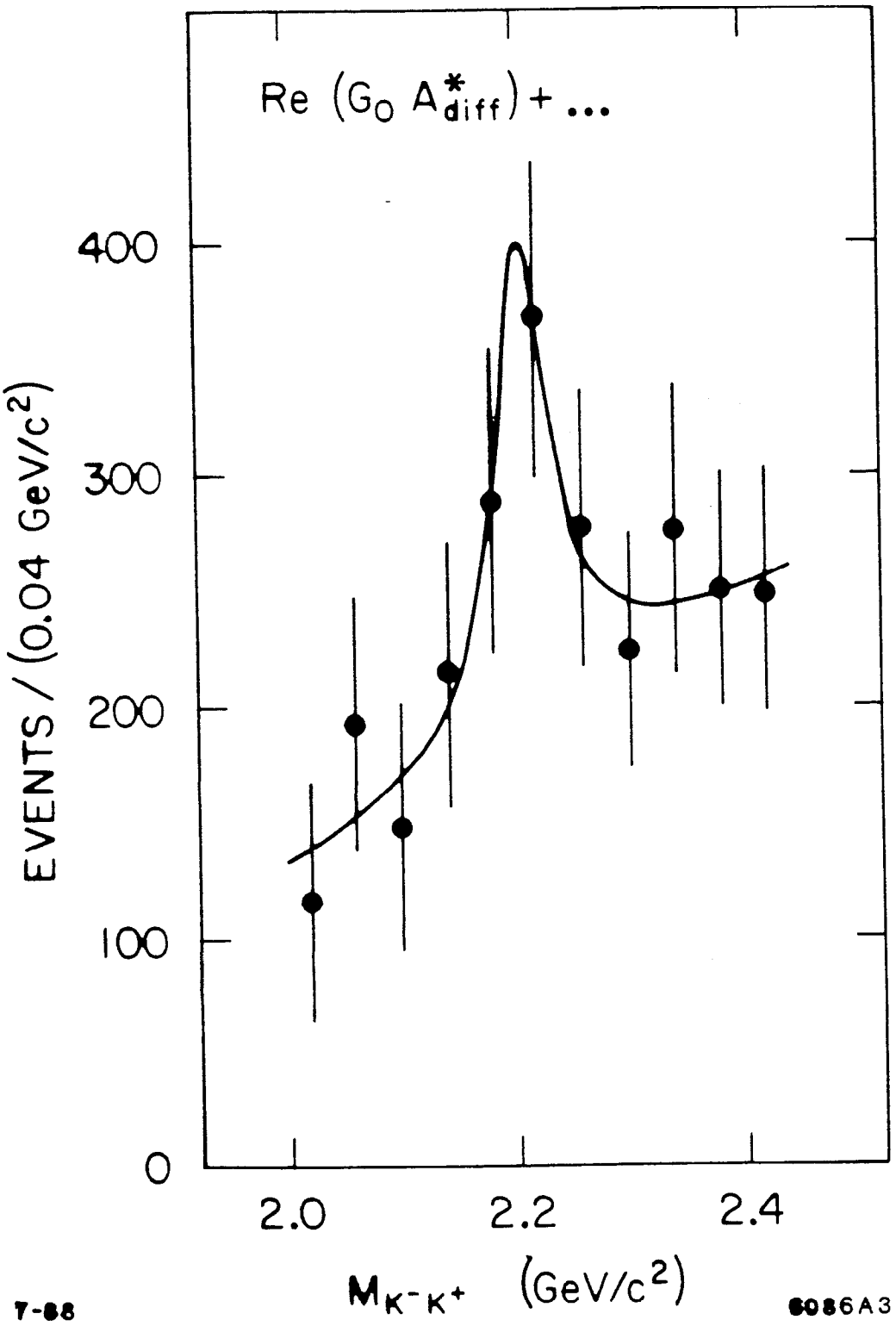
Re $(G_0 A^*_{diff}) + \ldots$
400
300
200
100
0
EVENTS / (0.04 GeV/c²)
2.0
2.2
2.4
$M_{K^-K^+}$ (GeV/c²)
7-68
6086A3

Fig. 10

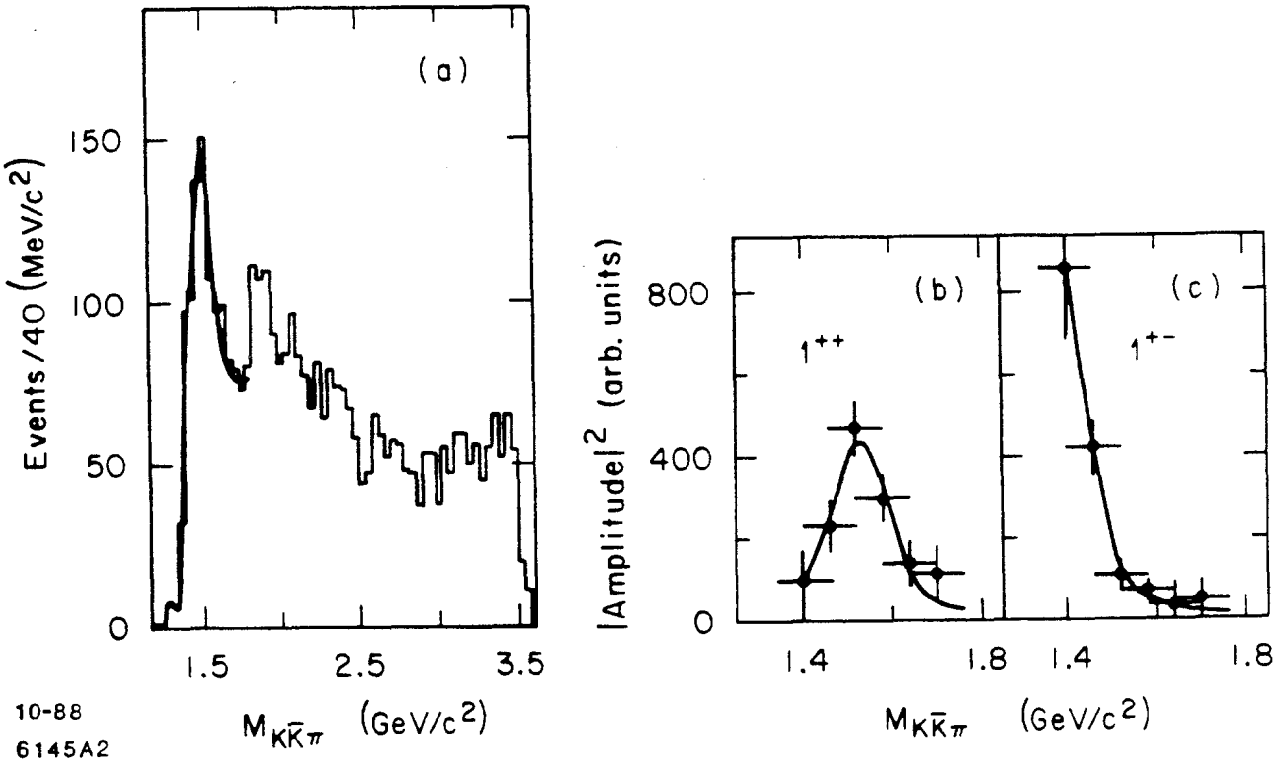
(a)
Events/40 (MeV/c²)
150
100
50
0
1.5
2.5
3.5
M_KK̄π (GeV/c²)
10-88
6145A2
(b)
1⁺⁺
(c)
1⁺⁻
|Amplitude|² (arb. units)
800
400
0
1.4
1.8
1.4
1.8
M_KK̄π (GeV/c²)

Fig. 11

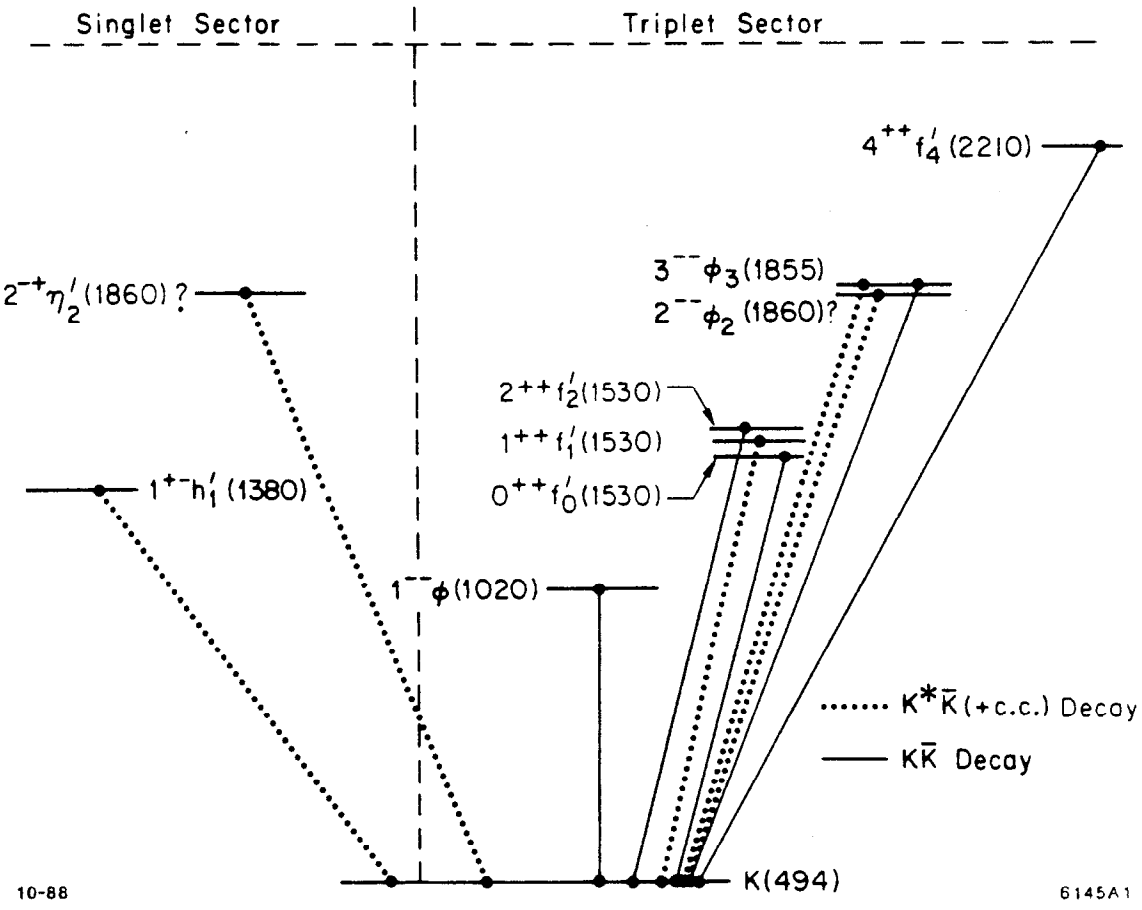
Singlet Sector
Triplet Sector
$4^{++} f_4'(2210)$
$3^{--} \phi_3(1855)$
$2^{--} \phi_2(1860)?$
$2^{-+} \eta_2'(1860)?$
$2^{++} f_2'(1530)$
$1^{++} f_1'(1530)$
$0^{++} f_0'(1530)$
$1^{+-} h_1'(1380)$
$1^{--} \phi(1020)$
$K^* \bar{K}$ (+c.c.) Decay
$K\bar{K}$ Decay
K(494)
10-88
6145A1

Fig. 12

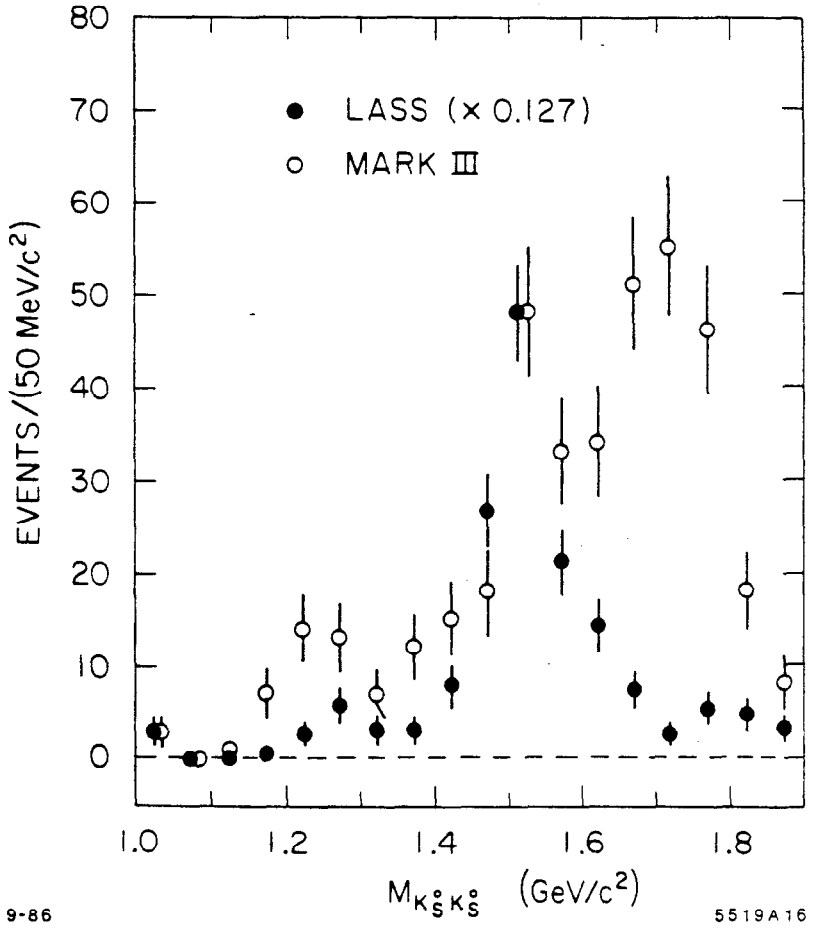
LASS (× 0.127)
MARK III
EVENTS/(50 MeV/c²)
80
70
60
50
40
30
20
10
0
1.0
1.2
1.4
1.6
1.8
$M_{K_S^0 K_S^0}$ (GeV/c²)
9-86
5519A16

Fig. 13

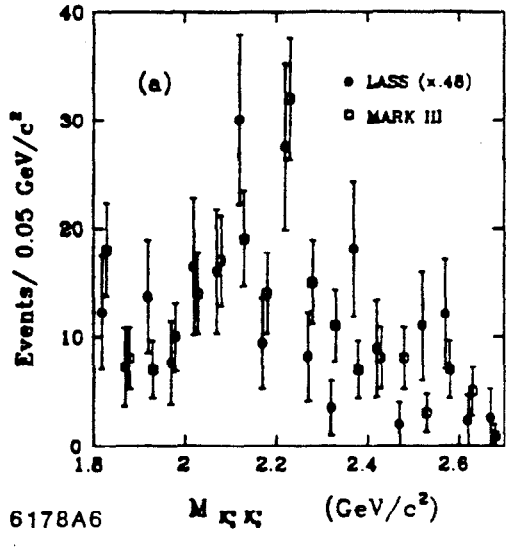
(a)
LASS (×.48)
MARK III
Events/ 0.05 GeV/c²
40
30
20
10
0
1.8
2
2.2
2.4
2.6
$M_{K^0 K^0}$ (GeV/c²)
6178A6

Fig. 14

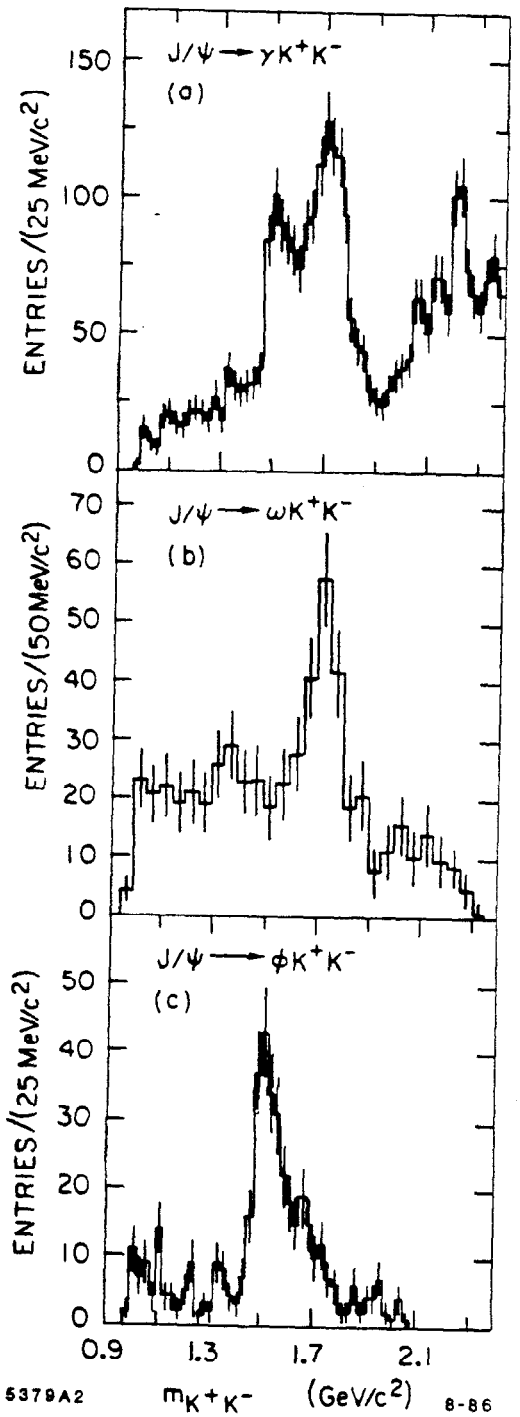
J/ψ → γK⁺K⁻
(a)
ENTRIES/(25 MeV/c²)
150
100
50
0
J/ψ → ωK⁺K⁻
(b)
ENTRIES/(50MeV/c²)
70
60
50
40
30
20
10
0
J/ψ → φK⁺K⁻
(c)
ENTRIES/(25 MeV/c²)
50
40
30
20
10
0
0.9
1.3
1.7
2.1
5379A2
m_K⁺K⁻ (GeV/c²)
8-86

Fig. 15